Aquat. Sci. 66 (2004) 421–429
1015-1621/04/040421-09
DOI 10.1007/s00027-004-0731-8

Aquatic Sciences

Research Article

UV-B radiation increases cell permeability and damages nitrogen incorporation mechanisms in *Nannochloropsis gaditana*

Cristina Sobrino[1, 2, *], Olimpio Montero[1] and Luis M. Lubián[1]

[1] Instituto de Ciencias Marinas de Andalucía (CSIC), Avda. República Saharaui, 2, ES-11510 Puerto Real, Cádiz, Spain
[2] Present address: Smithsonian Environmental Research Center, P.O. Box 28, Edgewater, Maryland 21037, USA

Received: 7 October 2003; revised manuscript accepted: 15 April 2004

Abstract. This study shows the response of *Nannochloropsis gaditana*, a marine nannoplanktonic species, exposed to UV radiation for 7 days. PAR, UV-A and UV-B ratios used were within the range likely to be observed in nature, a photoperiod of 12L:12D was maintained, and light irradiances were modified daily to promote cell acclimation. Growth, pigment content, internal nitrogen and carbon content, and photochemical efficiency using PAM fluorometry were assessed in nutrient replete cultures. Cell size, autofluorescence and cell permeability were analysed by flow cytometry. Results showed a cessation of growth after day 3 and a progressive decrease was observed in F_v/F_m values in cultures exposed to UV-B (plus UV-A and PAR). Flow cytometry analysis also demonstrated an increase in membrane permeability caused by UV-B damage. Cells that showed an increase in membrane permeability also exhibited a proportional decrease in cellular nitrogen content. The results support the conclusion that UV-B radiation can affect *N. gaditana* nitrogen incorporation mechanisms by direct damage or indirectly by damage to membrane structure and to the photosynthetic apparatus with resulting effects on energy and reductant demand. In contrast, the presence of UV-A radiation was beneficial to cells exposed to PAR plus UV-A when compared to those exposed to only-PAR from day 4. This response resulted in cells with a higher nitrogen content and without changes in membrane permeability.

Key words. Flow cytometry; membrane permeability; nitrogen incorporation; PAM fluorescence; ultraviolet radiation.

Introduction

The UV spectrum is divided into UV-C (100–280 nm), UV-B (280–315 nm)[1], and UV-A (315–400 nm) radiation. UV-C radiation as well as the radiation at shorter wavelengths is absorbed in the upper and middle atmosphere. Conversely, most of the UV-B and UV-A radiation reaches the Earth's surface. While the short wavelengths of UV-B always produce detrimental effects, long wavelengths of UV-A and PAR (400–700 nm) are able to inhibit some metabolic processes as well as take part in repair related mechanisms (used in a general sense to include all processes that counteract the inhibitory effect of UV such as resynthesis, reactivation, etc), depending on spectral conditions (Quesada et al.,1995; Pakker et al., 2000).

* Corresponding author e-mail: cristina.sobrino@icman.csic.es or sobrinoc@si.edu
Published on Web: November 3, 2004

[1] Limits for UV-B recommended by the Commission Internationale de l'Eclairage.

Ozone layer depletion results in an increase in UV-B radiation reaching the Earth's surface. The quantity of incidental UV radiation depends on several factors such as cloud cover and atmospheric aerosols, and its transmission into aquatic environments is, in addition, altered by variations in dissolved organic compounds and suspended particulates. The effect of UV radiation on marine phytoplankton is an important ecophysiological topic of interest owing to the fact that phytoplankton is the principal component of the carbon cycle and photoautotrophic organisms use light to convert carbon into organic compounds.

In phytoplanktonic organisms, the response to UV exposure varies according to the species (Karentz et al., 1991), depending on its sensitivity and repair capacity. Two cell components have been recognized as being particularly susceptible to damage by UV at the molecular level: nucleic acids (Setlow, 1974; Karentz et al., 1991; Buma et al., 1995) and the photosynthetic apparatus (Vincent and Neale, 2000, and references therein). However, there are several other molecules and processes affected simultaneously during exposure and it is sometimes difficult to attribute principal targets of damage. Moreover, it can be assumed that the different mechanisms involved have different kinetics of damage and repair, or that rates of damage and repair change with the alteration of external conditions, so finally the net response observed will rely on multiple factors, including time of exposure. Short-term assays (less than 24 h) are extremely useful for assessing cellular targets as well as their kinetics of damage and repair, however, long-term experiments can help reliably predict effects on communities (Montero et al., 2002).

The objective of the present study was to determine the effects of UV-B and UV-A on *Nannochloropsis gaditana*, a marine nannoplanktonic species, under long-term exposures. Growth, pigment content, and cellular carbon and nitrogen content were measured; photochemical efficiency was assessed by PAM fluorometry, and cellular permeability, size and autofluorescence were determined by flow cytometry.

Materials and methods

Organisms and culture conditions

Nannochloropsis gaditana Lubián (Eustigmatophyceae), strain 06/0201, cultures were provided by the Culture Collection of Marine Microalgae of The Instituto de Ciencias Marinas de Andalucía (CSIC, Cádiz, Spain). Aliquots for inoculation came from an aerated nutrient replete culture maintained in a growth chamber at 20 ± 2 °C and 86 µmol m^{-2} s^{-1}, the same PAR intensity as the maximum irradiance during UV exposure (18.7 W m^{-2} applying a conversion factor of 4.6 µmol J^{-1}). The growth medium was prepared by filtering and sterilizing seawater before enrichment with f/2 nutrients (Guillard and Ryther, 1962). Cultures were inoculated on the 4th day of growth, half way through the exponential growth phase. Cultures were nutrient-replete in order to observe exclusively the damage caused by UV radiation. The culture utilized for the inoculation showed $F_v/F_m = 0.71$. Initial density was 5.2×10^6 cell mL^{-1}.

Experimental set-up

Cultures (650 mL) were grown in UVR transparent Plexiglas cylinders (Plexiglas XT® 29080). Cylinder dimensions were 25 cm length × 6.5 cm diameter. Cylinders were wrapped with cellulose acetate cut-off filters Ultraphan 395 (Digefra GmbH. Ref. URUV), Folex 320 (Folex GmbH. Ref. 10155099) and Ultraphan 295 (Digefra GmbH. Ref. URT 100). Ultraphan 395 allows the transmission of radiation with wavelengths higher than 395 nm, Folex 320 allows wavelengths higher than 320 nm, and Ultraphan 295 allows wavelengths higher than 295 nm. The use of these filters generated three different spectral treatments: P (includes mainly PAR), PA (includes mainly PAR and UV-A) and PAB (includes PAR, UV-A and UV-B). The transmittance spectra for the filters mounted on a Plexiglas piece similar to that utilized for the cylinders are shown in Figure 1. For each spectral treatment, two cultures were exposed to the radiation in a growth chamber (Koxka, Hussman Koxka S.L., Spain) at 20 ± 2 °C. The cultures were maintained with continuous aeration to avoid prolonged self-shading between cells and CO_2 depletion.

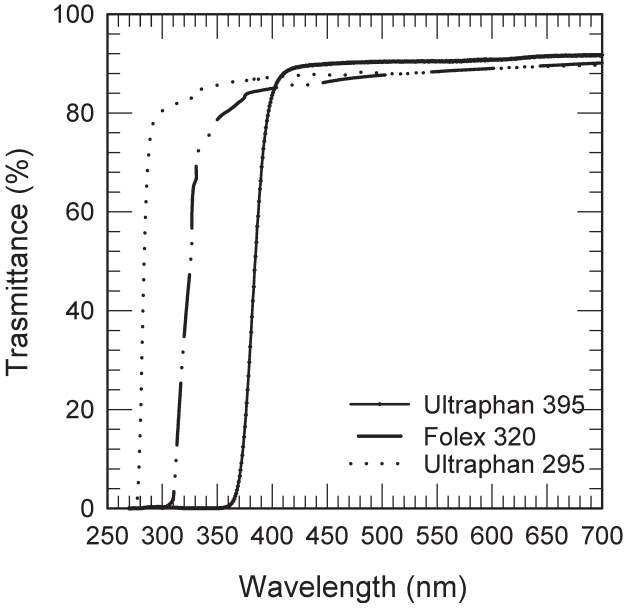

Figure 1. Transmittance spectra for the acetate cellulose filters Ultraphan 395, Folex 320 and Ultraphan 295 mounted on a Plexiglas piece similar to that used for the cylinders (100% transmittance).

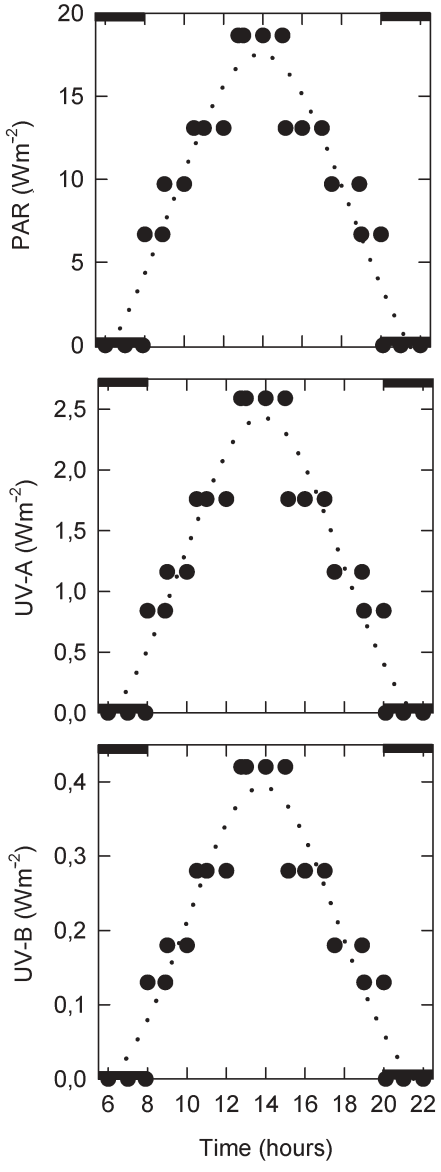

Figure 2. Time course of daily increase and decrease of PAR, UV-A and UV-B intensities used for *N. gaditana* exposure. *N. gaditana* cultures were maintained with photoperiod 12L:12D, with the light period from 8:00 to 20:00 hours. The dark period (Intensity = 0 Wm^{-2}), represented here by values before and after the light period, is indicated by black rectangles. Circles correspond to unweighted values (Table 1) and the dotted lines are regression functions.

PAR, UV-A and UV-B intensities were provided by Sylvania Daylight, Q-panel 340 and Philips TL 40 W/12 lamps, respectively. The irradiance for each treatment was measured in situ inside the cylinders with a spherical quantum sensor model P20HM33CM12KG (Zemoko, The Netherlands) connected to a LI-1000 data logger for PAR intensities, and a Dr. Gröbel RM-11 (UV- Elektronik GmbH, Ettlingen, Germany) broad band radiometer equipped with sensors for UV-A (315–400 nm, peak of relative response at 360 nm) and UV-B (280–315 nm, peak of relative response at 300 nm) measurements. Spectral irradiance from 300 nm to 800 nm was also measured with a LI-1800 UW spectroradiometer (LI-COR, Inc. Lincoln, Nebraska, USA) covered with the appropriate filters. Maximum PAR intensity used was 86 µmol m^{-2} s^{-1} (18.7 W m^{-2}) with UV-A and UV-B intensities then being calculated from this PAR value to simulate natural sunlight PAR:UV-A:UV-B ratios. Cultures were grown under a 12L:12D photoperiod. Moreover, during the experimental period, the cylinders wrapped with the acetate cellulose filters were daily covered and uncovered with 0, 1, 2 or 3 neutral density screens in order to simulate the increase and decrease in irradiance observed under natural solar exposures. Figure 2 shows the time course of light intensity for PAR, UV-A and UV-B radiation obtained by covering and uncovering the cylinders with the neutral screens and Table 1 shows the corresponding intensity values measured with the LI-1800 UW spectroradiometer. Weighted irradiance values shown in Table 1 were obtained by applying a Biological Weighting Function (BWF) previously determined for the inhibition of *N. gaditana* photosynthesis by UV radiation (Sobrino et al., unpublished data).

Cellular density and chlorophyll concentration

Cells were counted in a Neubauer haemacytometer. For each duplicate culture, three replicates were analysed. Growth rates (µ, day^{-1}) were calculated as the slope of ln N(t) vs. time during exponential growth phase, where N(t) is the cell concentration on day t. For the calculations, 5 to 6 different values were employed for each culture, except for the PAB treatment where densities employed were those from day 1 to 3 inclusive. Chlorophyll *a* concentration was measured in triplicate in aliquots concentrated by centrifugation (1726 g, 15 min, 4 °C). The pellet was extracted with 100% methanol and maintained in the dark overnight. After centrifugation, absorption of the supernatant was measured at the appropriate wavelengths according to the equation given by Talling and Driver (1963).

External nitrate concentration and cellular carbon and nitrogen content

The time course of nitrate concentration in the culture media was assessed following the protocol of Collos et al. (1999). For determination of cellular carbon and nitrogen content, cells contained in 200 mL culture were concentrated by centrifugation (12745 g, 5 min, 4 °C). In order to eliminate salt particles (which can increase the weight of the sample), pellets were then washed once with an isotonic 0.9% ammonium formate solution and re-suspended in 4 mL of this solution. The concentrate was maintained at –20 °C until freeze-drying. Before freeze-

Table 1. PAR, UV-A and UV-B intensities utilized for *N. gaditana* exposures measured with a LI- 1800 UW spectroradiometer. Results show unweighted (Wm^{-2}) and weighted (E^*_{inh}, dimensionless) irradiances for each spectral range. The measurements were performed by covering the Plexiglas with the filter Ultraphan 295, and with 0, 1, 2 and 3 neutral density screens. Weighted irradiance values were obtained by applying the Biological Weighting Function (BWF) for *N. gaditana* photoinhibition (Sobrino et al., unpublished results).

Neutral screens	Irradiance	Spectral range		
		PAR	UV-A	UV-B
0	Unweighted (Wm^{-2})	18.69	2.59	0.42
	Weighted (dimensionless)		0.18	0.49
1	Unweighted (Wm^{-2})	13.08	1.76	0.28
	Weighted (dimensionless)		0.12	0.33
2	Unweighted (Wm^{-2})	9.71	1.16	0.18
	Weighted (dimensionless)		0.09	0.21
3	Unweighted (Wm^{-2})	6.68	0.84	0.13
	Weighted (dimensionless)		0.06	0.15

drying, samples were homogenised and maintained at 60 °C overnight to volatilise the ammonium formate residuals (Utting, 1985). For each sample, 2 to 3 mg of sample biomass were weighted in a Mettler UM 3 microbalance. Carbon and nitrogen percentage (%C and %N) of the weighted biomass was then determined in a Carlo Erba autoanalyzer (Carlo Erba Strumentazione, Italia) using cyclohexanone 2,4-dinitrophenil hydrazone as standard. Analyses were performed in duplicate. Results are shown as %C and %N of dry weight.

Photosynthetic efficiency of PSII

The photosynthetic efficiency of PSII was measured as the chlorophyll fluorescence yield using the pulse amplitude modulated fluorimeter FMS1 (Hansatech, Kings Lynn, United Kingdom). Three (3) mL of culture were placed in a tube and adapted to the dark for 10 min. Analyses were performed in triplicate. The data are expressed as the maximum efficiency of excitation energy captured by PSII (F_v/F_m) and were calculated as $(F_m - F_0)/F_m$, where F_m is the maximum fluorescence obtained after a saturating light pulse and F_0 is the basal fluorescence (Schreiber et al., 1986). Maximum quantum yield was measured every day during the maximum light intensity period (cylinders uncovered). On day 3 of growth, triplicate measurements were also made before and after the dark period, when the Plexiglas tubes were covered with three neutral density screens. The experiment was concluded on day 7 when Fv/Fm values for PAB exposed cultures reached values close to zero.

Flow cytometry analysis

Samples for flow cytometric analysis were daily collected after the maximum light intensity period (cylinders covered with one neutral density screen) and analysed immediately using a FACScalibur flow cytometer (Beckton-Dickinson) equipped with a 488-nm excitation argon laser. For these samples the trigger was set on the red fluorescence (chlorophyll autofluorescence, FL3). For each spectral treatment three replicates from each culture were analysed in low flow for 30 seconds (6000–10000 events). Signals for Forward Angle Light Scatter (FSC), 90° angle side scatter or Side Light Angle Scatter (SSC), chlorophyll fluorescence (FL3) and membrane permeability measured as the fluorescein fluorescence emission (FL1) were recorded. Although SSC and FSC values are both widely utilized as good indicators of cell size, parallel experiments carried out with aliquots of various marine microalgae cultures showed that the SSC was the parameter that gave the best fit for the mean cell size (data not shown).

Membrane permeability was assessed using fluorescein diacetate (FDA. Ref. 20164-2. Sigma-Aldrich Co., USA). FDA is a hydrophobic and non-fluorescent dye that penetrates the cell plasma membrane due to its small size (mol. wt. 416). Once inside the cell, non-specific esterases break down the molecule resulting in fluorescent fluorescein which can be quantified by flow cytometry (Dorsey et al., 1989). Since these enzymes are involved in phospholipid turnover, the presence of active enzymes is normally correlated with metabolic activity (Dorsey et al., 1989). However, in cases in which the cellular envelope does not allow the incorporation of the stain the fluorescence is also indicative of cell permeability. As *N. gaditana* has a strong cellular wall, the fluorescence emission increases exponentially until reaching a maximum only after more than 5 hours of incubation with the FDA. As measurements performed after long incubation times can involve losses of fluorescence as well as changes in cell physiological status, the incubation time used for the present study was fixed at 20 min. This time allows stain incorporation and subsequent fluorescence emission pro-

portional to cell permeability, but without a loss of fluorescence. FDA was dissolved in HPLC-grade acetone to yield a final FDA solution concentration of 1 mg mL^{-1}. Ten (10) µL of stain solution was added to 1 mL aliquots of the *N. gaditana* cultures exposed to each spectral treatment and vortexed gently (Faber et al., 1997). Samples were maintained in the dark for 20 min for stain incorporation until fluorescence emission was registered by the FL1 photomultiplier. Data for cell parameters were computed with CellQuest software (Beckton-Dickinson).

Statistical analysis

The results obtained from P, PA and PAB spectral treatments were analysed by a one way ANOVA followed by a Student-Newman-Keuls post test. Significant differences ($p < 0.05$) with P spectral treatment are shown as *, and those with PA spectral treatment are shown as †.

Results

Cell density and pigment content

Cells from cultures exposed to the P and PA spectral treatment divided exponentially without significant differences between treatments. For these cultures maximal densities were reached on day 7 showing values of 25.5×10^6 cells mL^{-1} and 37.1×10^6 cells mL^{-1}, respectively. In cells exposed to the PAB treatment, growth rates were significantly lower attaining maximal cell densities of 6.64×10^6 cells mL^{-1} on day 3 (Table 2).

Cellular pigment content increased with time in all cultures with the PAB treatment showing highest cellular chlorophyll *a* value for day 4 (Table 2). From day 5 to 6 chlorophyll concentration decreased in cells exposed to the PAB treatment and on day 6 was not different to the P and PA exposed cultures.

Carbon and nitrogen content

Nitrate concentrations in the culture media decreased from 1822 µM to 1591 ± 57 µM and 1505 ± 17 µM by day 6 for the cultures exposed to the P and PA treatments, respectively. No significant changes were observed in nitrate concentration in cultures exposed to the PAB treatment (Fig. 3A).

Cellular carbon (C) and nitrogen (N) content increased from day 4 to day 7 in the P and PA treatment cultures, decreasing in the PAB treatment. Cells exposed to the PA treatment exhibited higher C and N values than the P treatment cells with the highest nitrogen content. The PAB treatment cells showed the highest carbon content but the lowest nitrogen content on day 4 ($p < 0.05$) (Fig. 3B).

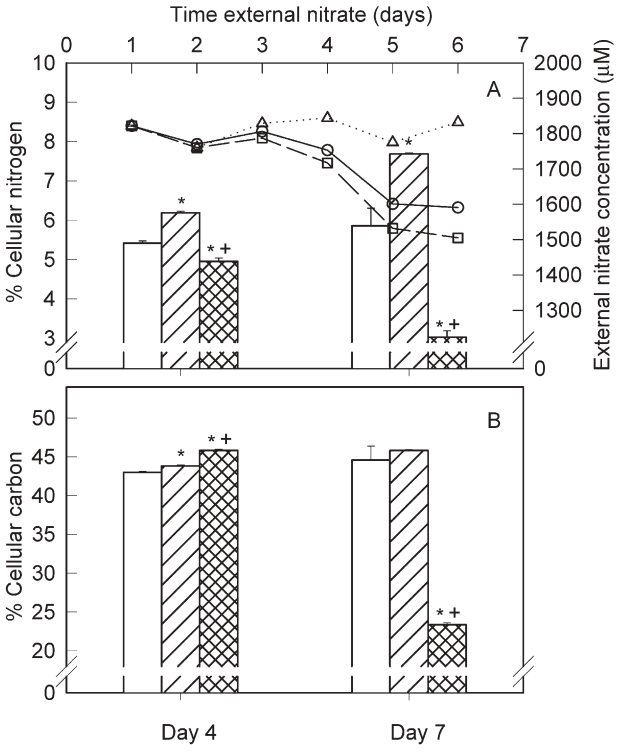

Figure 3. Mean values ± SE of (A) cellular nitrogen content (bars) and external nitrate concentrations (symbols), and (B) cellular carbon content, of *N. gaditana* cultures exposed to the P, PA and PAB spectral treatments. Symbols: circle and open bars = P treatment, square and dashed bars = PA treatment, and triangle and crossed bars = PAB treatment. Significant differences ($p < 0.05$) with P spectral treatment are shown as *, and those with PA spectral treatment are shown as †.

Table 2. Growth rates (µ, day^{-1}), maximal density attained ($N \times 10^6$ cells mL^{-1}) and cellular pigment content (ng Chl *a* (10^6 cells)$^{-1}$) of *N. gaditana* cultures exposed to the P, PA and PAB spectral treatments. Values shown in the table are means ± SE. Significant differences ($p < 0.05$) with P spectral treatment are shown as *, and those with PA spectral treatment are shown as †.

	Day	P	PA	PAB
µ (d^{-1})		0.29 ± 0.00	0.32 ± 0.03	0.08 ± 0.02
Maximal cell density ($N \times 10^6$ cells mL^{-1})		25.48 ± 2.92	37.10 ± 3.80	6.64 ± 0.61*†
Chlorophyll *a* (ng Chl *a* (10^6 cells)$^{-1}$)	4	47.50 ± 8.10	44.30 ± 0.20	74.20 ± 9.00*†
	6	74.30 ± 0.50	68.70 ± 8.80	64.50 ± 2.50

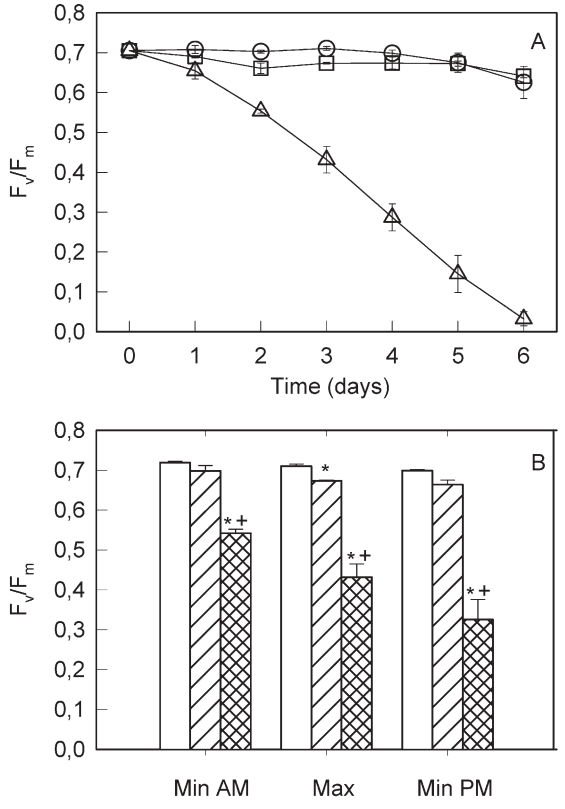

Figure 4. Time course of F_v/F_m mean values ± SE of *N. gaditana* cultures exposed to the P, PA and PAB spectral treatments. (A) Measurements performed daily during maximal light intensity period (cylinders uncovered). (B) Measurements performed during day 3, just before and after the dark period (Min AM and Min PM, respectively. Cylinders covered with three neutral screens) and during maximal light intensity period (Max. Cylinders uncovered). Symbols: circle and open bars = P treatment, square and dashed bars = PA treatment, and triangle and crossed bars = PAB treatment. Significant differences ($p < 0.05$) with P spectral treatment are shown as *, and those with PA spectral treatment are shown as †.

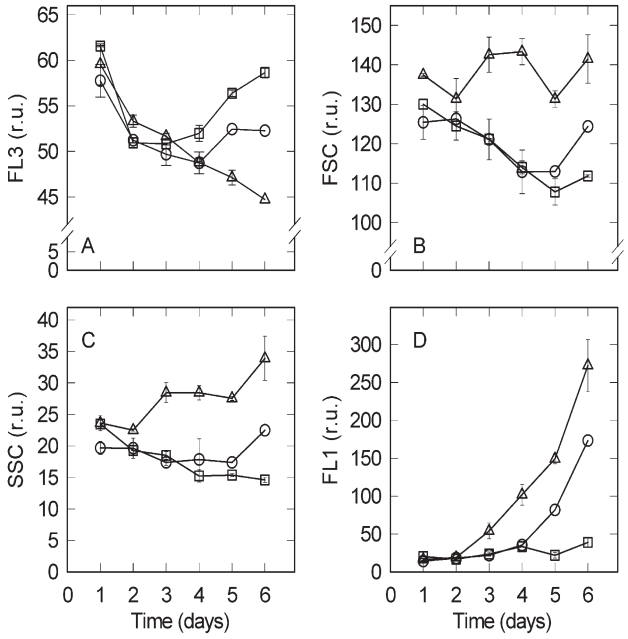

Figure 5. Time course of values obtained from flow cytometric analysis of *N. gaditana* cultures exposed to the P, PA and PAB spectral treatments. The symbols represent mean values ± SE of A) chlorophyll autofluorescence (FL3), B) and C) cell volume represented by the Side Angle Light Scatter (SSC) and Forward Light Scatter (FSC), and D) cell permeability measured as the fluorescein fluorescence emission (FL1) Symbols: circle = P treatment, square = PA treatment, and triangle = PAB treatment.

Chlorophyll fluorescence

During the experimental period the F_v/F_m mean value was 0.69 ± 0.03 for the P treatment cultures. Fv/Fm value of the PA treatment cultures was approximately constant (0.64 ± 0.02) over the entire exposure period and slightly lower than that of the P cultures until day 4, at which time F_v/F_m dropped in the P treatment exposed cultures (Fig. 4A). F_v/F_m decreased in the cultures exposed to the PAB treatment with the exposure time, reaching values close to zero by day 6. The rate of decrease was lower between day 0 and day 1, then increased from day 1 to 2 becoming constant from day 2 to 6, the F_v/F_m values decreasing linearly.

A similar pattern of variation in F_v/F_m was observed between the different treatments over the photoperiod illumination cycle on day 3 (Fig. 4B). F_v/F_m values of the PAB treatment cultures decreased linearly with time of exposure. In contrast, F_v/F_m values of the P treatment cultures did not show differences during the day and those for cultures exposed to the PA treatment were lower during maximum light intensities but recovered with further lowering of light intensity.

Flow cytometry

Flow cytometry analysis results showed that after decreasing from day 1 to 3 in the PA treatment cultures, and day 1 to 4 in the P treatment cultures, FL3 increased in these cultures (Fig. 5A). Autofluorescence (FL3 signal) was significantly higher in the PA cultures than in the P cultures from day 4. Cells exposed to the PAB treatment showed FL3 values which decreased progressively with time of exposure, although with similar values to those of cells exposed to the P and PA treatments until day 4 (Fig. 5A).

SSC and FSC values showed that from day 1 to 4, P and PA treatments cell size decreased, while the PAB treatment increased cell size until the end of the experiment. From day 4 to 6, P treatment cell size also increased. On days 5 and 6 the size of the PAB culture cells was significantly greater than the size of the P treatment cells, and both were larger than those exposed to the PA treatment (Figs. 5B, C).

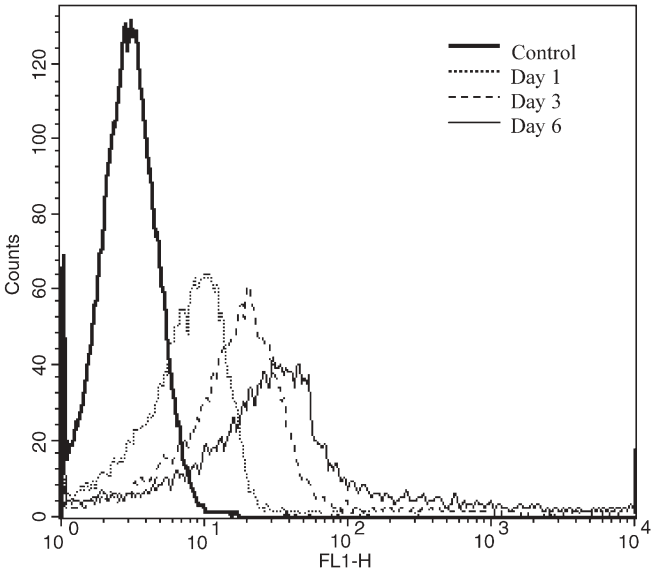

Figure 6. *Nannochloropsis gaditana* histograms obtained from flow cytometric analysis for membrane permeability assessment (FL1). Control histogram corresponds to non-stained PAR exposed cells, and Day 1, Day 3 and Day 6 corresponds to cells exposed to PAB treatment the days 1, 3, and 6 respectively, and maintained with FDA during 20 minutes.

Membrane permeability, indicated by the FL1 signal, increased exponentially during the experimental period in cells exposed to the PAB treatment, these cells showing values higher than those exposed to both P and PA treatments, after day 2 (Fig. 5D). Cells exposed to the P treatment showed a similar pattern in fluorescence emission to those exposed to the PAB treatment after day 4. Membrane permeability in PA treatment cells was approximately constant throughout the experimental period (Fig. 5D). Membrane permeability in PAB exposed cells was significantly higher than in the PA and P exposed cells after day 2; however, it was only higher than the PA exposed cells on day 6. On days 5 and 6 membrane permeability in the P exposed cells was also significantly higher than in the PA exposed cells (Fig. 5D).

Figure 6 shows FL1 signal histograms of *N. gaditana* cells exposed to the PAB spectral treatment on days 1, 3 and 6. The control histogram corresponds to unstained cells of a PAR exposed culture that did not show changes in permeability. Figure 6 shows that cell permeability of the cells exposed to the PAB treatment increased over the experimental period as seen by the increase in fluorescence emission (as indicated by signal displacement to the right on the X axis). As the time of sample analysis was the same for each sample, peak height decreased from day 1 to day 6 due to the decrease in cell number caused by UV-B damage (decrease of peak height).

Discussion

Although a large number of studies have focused on the damage produced by UVR on several cellular targets, little is known about the role that other processes such as acclimation or repair play in the long term (Veen et al., 1997; Zudaire and Roy, 2001). Many studies of UV related damage have been carried out under short-term exposures and UVR regimes that differed quantitatively, as well as qualitatively, from natural sunlight. Taking this into account, a special effort was made in this study to simulate the daily increase and decrease in irradiance which promotes cell photoacclimation. Furthermore, although light intensities used in the present study do not accurately reproduce PAR:UV-A:UV-B sunlight ratios, they are however within the range likely to be observed in nature. In addition, the experiments were developed under moderate intensities where UV-B exposures should not produce acute damage to cells. UV-B radiation was also accompanied by PAR and UV-A intensities responsible for repair activation processes related to UV-B damage (Quesada et al.,1995; Pakker et al., 2000) and maximum PAR intensities employed did not produce photoinhibition, as deduced from the F_v/F_m values. However, *N. gaditana* cultures exposed to UV-B (plus PAR and UV-A) did not grow after 3 days of exposure.

The fact that cultures exposed to the PAB treatment continued to increase in both size and pigment content, as well as showing higher carbon content than cells exposed to the P and PA treatments, demonstrated that the metabolic processes involved were not totally interrupted despite disruption of cell division (Buma et al., 1996). An increase in cell size is often related with the duplication of cell content, without cell division, due to UV-B damage (Karentz et al., 1991; Buma et al., 1996; Buma et al., 2000). Cellular nitrogen content however, was significantly lower in cultures exposed to the PAB treatment due to a lack of external nitrogen incorporation. This was in contrast to the P and PA treatments where external nitrogen was incorporated, with cells exposed to the PA treatment having the highest nitrogen contents.

F_v/F_m values, accepted as a good indicator of photosynthetic capacity (Schreiber et al., 1994) were similar for cultures exposed to the P and PA treatments. In cultures exposed to PAB, these values decreased almost linearly until reaching values close to zero by day 6. However, despite this progressive decay in UV-B exposed cultures, photosynthetic yields on day 3 were not so low as to provoke the disruption of the cell cycle ($F_v/F_m = 0.45$). Fv/Fm measurements on day 3 showed values typical of stressed cells (65% of the control) but do not explain the lack of cell division. These results provide evidence that other molecules sensitive to UV-B, besides PSII, have also to be considered in order to explain the response observed in the PAB-exposed cells. Furthermore, F_v/F_m de-

cay did not show kinetics similar to those recorded from typical UV-B damaged short-time exposed samples, where exposure response shows an early linear time dependence, before a transition to a time-independent, asymptotic equilibrium (Cullen and Neale, 1997; Heraud and Beardall, 2000). During short-term exposures, the response of phytoplanktonic organisms to photoinhibition by UVR is determined by their kinetics of damage and repair rates (Cullen and Neale, 1997; Heraud and Beardall, 2000; Neale, 2000). When the rate of repair is low, or practically negligible, repair does not counteract damage and the response is exclusively damage-dependent. The quantity of damaged targets is then "time-dependent" and consequently, photosynthetic rates decrease as a linear function of cumulative exposure (Neale et al., 1998; Neale, 2000). In contrast, when repair is proportional to damage, the rate of photosynthesis decays in response to UV exposure and within 30 minutes reaches a steady state consistent with a dynamic balance between damage and repair (Lesser et al., 1994; Heraud and Beardall, 2000; Neale et al., 1998). In the present study, the fact that F_v/F_m values decreased almost linearly as a function of time of exposure in the PAB treatment indicates a negligible rate of repair from day 2. In previous short-term studies, when repair is inhibited, e.g. by antibiotics, damage accumulates and photosynthetic efficiency decreases rapidly showing values close to 0.2 in less than 120 minutes (Heraud and Beardall, 2000). However, in this long-term study the decrease in the photosynthetic efficiency was slower and apparently preceded by two different phases, each of 24 h. The initial phase of the exposure, from day 0 to 1, showed a time-independent behaviour and was followed by a transition phase from day 1 to 2. Finally, the latter linear phase was described by the cumulative exposure due to the lack of repair (day 2 to 6).

It has been reported that UVR is able to damage membranes, directly by lipid peroxidation or indirectly by protein channel inhibition or by cell wall degradation (Murphy, 1983, and references therein). In the present study, the occurrence of UV-B induced structural changes in *N. gaditana* cellular envelope under the PAB treatment was reflected by the exponential rise in fluorescence emission due to FDA incorporation. Contrary to previous studies where FDA flow cytometric analyses has been used as a method for cell viability (Dorsey et al., 1989; Faber et al., 1997), for *N. gaditana*, due to its strong cellular wall, fluorescence emission is related to cell permeability (Lubián and Cañavate, 2001). If the cellular envelope is not damaged, the FDA does not penetrate into the cell and there is no fluorescence emission. When cells are damaged the cell permeability increases, increasing the probability for fluorescence emission which is in contrast to the expected response (Lubián and Cañavate, 2001).

Although Fv/Fm values for P exposed cultures demonstrated that the photosynthetic apparatus was not damaged, during days 5 and 6 cell permeability increased exponentially under only-PAR exposures, similar to that which occurred under the PAB treatment. In contrast, the PA treatment was not detrimental to the cells. By the end of the experiment cells in the PA treatment had a smaller cell size, lower membrane permeability and higher autofluorescence and cellular nitrogen than cells exposed to the P treatment. Hence, the results show the importance of high PAR intensities and UV-A on species such as *N. gaditana* in which the activation of protective and repair mechanisms related to high PAR intensities such as xanthophylls de-epoxidation and D1 turnover (Lubián and Montero, 1998; Figueroa et al., 1997; Neale, 2001) and UV-A (Quesada et al., 1995) play an important role.

Several studies have described an inhibitory effect of UV-B on inorganic nitrogen incorporation (Döhler, 1985; Döhler and Hagmeier, 1997) as well as the increase in sensitivity in nutrient-deficient cultures due to less efficient repair (Cullen and Lesser, 1991; Litchman et al., 2002). Both previous and present results support the hypothesis that the response observed in *N. gaditana* cultures exposed to the PAB treatment is also due to UV-B damage caused to the cellular membrane, apart from other cellular targets of the UV radiation. However, further experiments are necessary to reach more specific conclusions about the mechanism and the molecular targets of damage. UV-B damage to the membrane could also have affected nitrogen incorporation mechanisms, thus leading to the lack of external nitrogen incorporation and the decrease in the cellular nitrogen content. Subsequently, a lack of nitrogen would inhibit nucleic acid synthesis and essential protein turnover, so damage to membranes would contribute *a posteriori* to the decrease in the rate of repair, slowly and progressively decreasing photosynthetic efficiency. Concomitantly, reduced photosynthesis causes a decrease in ATP and NADPH production demanded by nitrogen and carbon assimilation mechanisms. This fact would also impose constraints on structural protein synthesis leading to a deficient membrane performance, and finally contributing to the synergistic interplay between the different UV damaging effects.

Acknowledgments

This work was financially supported by the Ministry of Science and Technology of Spain (MSTS) through project AMB 97-1021-C02-02, and by an individual fellowship granted to C S. (PN97 30668168). Authors thank Dr. Félix L. Figueroa (University of Málaga) for graciously providing the LI-1800 spectroradiometer, Neil Ruane and Brad Morris for the English revision and three anonymous reviewers for providing helpful suggestions.

References

Buma, A. G. J., E. J. Van Hannen, L. Roza, M. J. W. Veldhuis and W. W. C. Gieskes, 1995. Monitoring UV-B-induced DNA damage in individual diatom cells by immunofluorescencent thymine dimer detection. J. Phycol. **31:** 314–321.

Buma, A. G. J., H. J. Zemmelink, K. Sjollema and W. W. C. Gieskes, 1996. UV-B radiation modifies protein and photosynthetic pigment content, volume and ultraestructure of marine diatoms. Mar. Ecol. Prog. Ser. **142:** 47–54.

Buma, A. G. J, T. Van Oijen, W. Van de Poll, M. J. W. Veldhuis and W. W. C Gieskes, 2000. The sensitivity of *Emiliania huxleyi* (Prymnesiophyceae) to UV-B radiation. J. Phycol. **36:** 296–303.

Collos, Y., F. Mornet, A. Sciandra, N. Waser, A. Larson. and P. J. Harrison, 1999. An optical method for the rapid measurement of micromolar concentrations of nitrate in marine phytoplankton cultures. J. Appl. Phycol. **11:** 179–184.

Cullen, J. J. and M. P. Lesser, 1991. Inhibition of phytoplankton photosynthesis by ultraviolet radiation as a function of dose and dosage rate. Mar. Biol. **111:** 83–90.

Cullen, J. J and P. J. Neale, 1997. Biological weighting functions for describing the effects of ultraviolet radiation on aquatic systems. In: D.-P. Häder (ed.), The Effects of Ozone Depletion on Aquatic Ecosystems, Landes, Austin, pp. 97–118.

Döhler, G., 1985. Effect of UV-B radiation (290–320nm) on the nitrogen metabolism of several marine diatoms. J. Plant. Physiol. **11:** 391–400.

Döhler, G. and E. Hagmeier, 1997. UV effects on pigments and assimilation of ^{15}N-ammonium and ^{15}N-nitrate by natural marine phytoplankton of the north sea. Bot. Acta **110:** 481–488.

Dorsey, J., C. M. Yentsch, S. Mayo and C. McKenna, 1989. Rapid analytical technique for the assessment of cell metabolic activity in marine microalgae. Cytometry **10:** 622–628.

Faber, M. J., L. M. J. Smith, H. J. Boermans, G. R. Stephenson, D. G. Thompson and K. R. Solomon, 1997. Cryopreservation of fluorescent marker-labelled algae (*Selenastrum capricornutum*) for toxicity testing using flow cytometry. Environ. Toxicol. Chem. **16(5):** 1059–1067.

Figueroa, F. L., C. Jiménez, L. M. Lubián, O. Montero, M. Lebert and D.-P. Häder, 1997. Effects of high irradiance and temperature on photosynthesis and photoinhibition in *Nannochloropsis gaditana* Lubián (Eustigmatophyceae). J. Plant Physiol. **151:** 6–15.

Guillard, R. R. L. and J. H. Ryther, 1962. Studies on marine planktonic diatoms 1. *Cyclotella nana* Hustedt and *Denotula confervaceae* (Cleve). Gran. Can. J. Microbiol. **8:** 229–239.

Heraud, P. and J. Beardall, 2000. Change in chlorophyll fluorescence during exposure of *Dunaliella tertiolecta* to UV radiation indicate a dynamic interaction between damage and repair processes. Photosyn. Res. **63:** 123–134.

Karentz, D., J. E. Cleaver and D. L. Mitchell, 1991. Cell survival characteristics and molecular responses of Antarctic phytoplankton to UV-B radiation. J. Phycol. **27:** 326–341.

Lesser, M. P., J. J. Cullen and P. J. Neale, 1994. Carbon uptake in a marine diatom during acute exposure to UV-B radiation: relative importance of damage and repair. J. Phycol. **30:** 183–192.

Litchman, E., P. J. Neale and A. T. Banaszak, 2002. Increased sensitivity to ultraviolet radiation in nitrogen-limited dinoflagellates: Photoprotection and repair. Limnol. Oceanogr. **47(1):** 86–94.

Lubián, L. M. and J. P. Cañavate, 2001. Obtención de biomasa concentrada de microalgas marinas para su utilización como alimento larvario de especies marinas, in Pesca y Acuicultura. In: Junta de Andalucía (ed.), Serie Acuicultura, pp. 1–49. In spanish.

Lubián, L. M. and O. Montero, 1998. Excess light-induced violaxanthin cycle activity in *Nannochloropsis gaditana* (Eustigmatophyceae): effects of exposure time and temperature. Phycologia **37(1):** 16–23.

Montero, O., M. Klisch, D.-P. Häder and L. M. Lubián, 2002. Comparative Sensitivity of Seven Marine Microalgae to Cumulative Exposure to Ultraviolet-B Radiation with Daily Increasing Doses. Bot. Mar. **45:** 305–315.

Murphy, T. M., 1983. Membranes as targets of ultraviolet radiation. Physiol. Plant. **58:** 381–388.

Neale, P. J., 2000. Spectral weighting functions for quantifying the effects of ultraviolet radiation in marine ecosystems. In S. J. de Mora, S. Demers and M. Vernet (eds.), The effects of UV radiation on marine ecosystems, Cambridge Univ. Press, Cambridge, pp. 73–100.

Neale, P. J., 2001. Modelling the effects of ultraviolet radiation on estuarine phytoplankton production: impact of variations in exposure and sensitivity to inhibition. J. Photochem. Photobiol. B: Biology **62:** 1–8.

Neale, P. J., A. T. Banaszak and R. J. Jarriel, 1998. Ultraviolet sunscreens in *Gymnodinium sanguineum* (Dinophyceae): Mycosporine-like amino acids protect against inhibition of photosynthesis. J. Phycol. **34:** 928–938.

Pakker, H., C. A. C. Beekman and A. M. Breeman, 2000. Efficient photoreactivation of UVBR-induced DNA damage in the sublittoral macroalga *Rhodymenia pseudopalmata* (Rhodophyta). Eur. J. Phycol. **35:** 109–114.

Quesada, A., J. Mouget and W. F. Vincent, 1995. Growth of Antarctic cyanobacteria under ultraviolet radiation: UV-A counteracts UV-B inhibition. J. Phycol. **31:** 242–248.

Schreiber, U., W. Bilger and C. Neubauer, 1994. Chlorophyll fluorescence as a nonintrusive indicator for rapid assessment of in vivo photosynthesis. In: E. D. Schulze and M. M. Caldwell (eds.), Ecophysiology of Photosynthesis, Springer, Berlin, 1994, pp. 49–70.

Schreiber, U., U. Schliwa and W. Bilger, 1986. Continuous recording of photochemical and non-photochemical chlorophyll fluorescence quenching with a new type of modulation fluorometer. Photosyn. Res. **10:** 51–62.

Setlow, R. B., 1974. The wavelengths in sunlight effective in producing skin cancer: a theoretical analysis. Proc. Natl. Acad. Sci. USA. **71:** 3363–3366.

Talling, J. F. and D. Driver, 1963. Some problems in the estimation of chlorophyll a in phytoplankton. Proc. Conference of Primary Productivity Measurement, Marine and Freshwater. Hawaii, 1961, U.S. Atomic Energy Comm. TID–7633, pp. 142–146.

Utting, S. D., 1985. Influence of nitrogen availability on the biochemical composition of three unicellular marine algae of commercial importance. Aquacult. Eng. **4:** 175–190.

Vincent, W. F. and P. J. Neale, 2000. Mechanisms of UV damage to aquatic organisms. In S. J. de Mora, S. Demers and M. Vernet (eds.), The effects of UV radiation on marine ecosystems, Cambridge Univ. Press, Cambridge, pp. 149–176.

Veen, A., M. Reuvers and P. Rونçak, 1997. Effects of acute and chronic UV-B exposure on a green algae: a continuous culture study using a computer-controlled dynamic light regime. Plant Ecol. **128:** 28–40.

Zudaire, L. and S. Roy, 2001. Photoprotection and long-term acclimation to UV radiation in the marine diatom *Thalassiosira weissflogii*. J. Photochem. Photobiol. B: Biol. **62:** 26–34.